Adaptation of the Field of View of a Cardiac SPECT System in Real Time

M. Bernard, G. Montemont, S. Stanchina, Stéphane Mancini, Loick Verger

Adaptation of the Field of View of a Cardiac SPECT System in Real Time

M. Bernard[1], G. Montémont[1], S. Stanchina[1], S. Mancini[2] and L. Verger[1]
Univ. Grenoble Alpes, F-38000 France
[1]*CEA LETI MINATEC Campus, F-38054 Grenoble France*
[2]*TIMA laboratory, UGA, F-38031 Grenoble France*

I. Introduction

Single Photon Emission Tomography (SPECT) is well known to be limited by the trade-off between spatial resolution and sensitivity, fixed by the collimator. This trade-off can be enhanced by adapting the field of view of the system to the imaged object. Thanks to the compactness of CdZnTe based detectors, adaptable configurations are achievable, in particular, dynamic positioning of detection heads. Dynamic adaptation of the field of view during the acquisition depending on the object characteristics can improve the image quality obtained with the same amount of photons. This adaptability is challenging because it needs real-time processing of the reconstruction and real-time reconfiguration. A previous work [1] proposed an algorithmic solution to process the reconstruction online.

The aim of the present study is to use this reconstruction method to reconfigure the system in real time, depending on the estimation. The reconstruction process uses normalization factors for each voxel of the object, in order to correct the non uniformity of the visibility of the system in the object. For a static system, these coefficients are computed upstream. But in a dynamic configuration, these normalization coefficients change with the configuration. Therefore, the reconfiguration of the system implies the computation of normalization factors in real time. Another issue raised by the dynamic reconfiguration is the computation of a criteria depicting the amount of information brought by all possible configurations, in order to select the most effective one for the next step. This work proposes a normalization technique achievable in real-time to empower the adaptivity of the geometrical configuration. Then, it proposes a criteria based on the Detective Quantum Efficiency, an approximation of Fisher information fast to compute. It concludes with a prompt comparison between a classic acquisition and an adapted one.

II. System Configuration

A. Detector and Collimation

A $40 \times 40 \times 5$ mm CZT detector composed of 256 anodes (2.5×2.5 mm each) and its readout system [2] is used to detect emitted gamma rays. The resolution of the detector is refined using 3D-positioning of measurements inside the detector [3] [4]. We use a 20-mm-high collimator, with a pitch of 2.5 mm, and square 1.5- mm-wide holes placed at 15 mm from the surface of the detector. This configuration enables a sensitivity of 1.5×10^{-4} and a spatial resolution of 8 mm at 15 cm from the object.

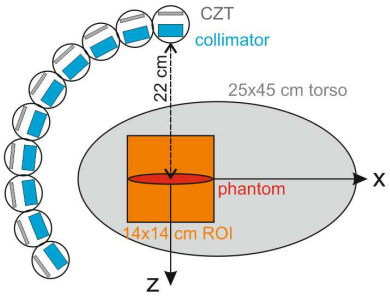

Fig. 1. Flexible configuration for cardiac imaging used in this study.

B. Geometrical Configuration

We study the case of a flexible cardiac imaging system with 10 independent detection heads placed on a 120-degrees-wide arc around the patient, at 220 mm from the center of the object to be imaged, in the spirit of the architecture proposed by Spectrum Dynamics (Fig. 1). Each head can rotate on itself independently from others along the y-axis with 21 determined orientations that covers 40 degrees with steps of 2 degrees. Heads are made of 4 modules placed on the same line, their size is thus 40×160 mm. Using this flexible configuration, heads can be oriented a longer time to the regions of the body which bring the most information.

C. General Method and Reconstruction Algorithm

The adaptation of heads orientations is made from the result of the reconstruction from previous measurements. As illustrated in Fig. 2, the previous intermediate estimation of the object is used to determine the information brought by each orientation and each head of the system. The time spent by one head orientation is then computed depending on the distribution of information of that head among all the possible orientations.

A more accurate configuration empowers a better acquisition of more informative measurements, which leads to a more exact estimation. The system can then be re-adapted depending on this new estimation, and so on.

DOI: 10.12059/Fully3D.2017-11-3202017

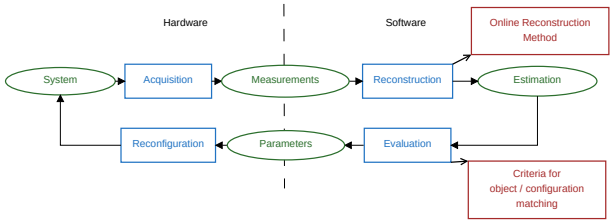

Fig. 2. Process used to dynamically adapt the configuration of the system.

Because the adaptation of the configuration is made depending on previous estimations of the object, an intermediate estimation of the object must be calculated during the acquisition, and thus requires real-time computing of the reconstruction. A previous study inspired from OSEM [5] proposed an algorithm (Partial LMMLEM-MC) using list mode MLEM [6]. Usual OSEM algorithms sort events depending on their location. Because of the temporal modifications of this system, we propose to sort events depending on their acquisition time. Each group of measurements is the result of one configuration of the system. Groups are used for the update of the next intermediate estimation of the object.

Intermediate estimation $O^{(g+1)}$ from the $(g+1)^{th}$ group is obtained from temporal group $\mathcal{K}^g$ of events k using the following update formula:

$$O_o^{(g+1)} = O_o^{(g)} + \frac{O_o^{(g)}}{N^{(g)}(o)} \times \sum_{k \in \mathcal{K}^g} \frac{\mathbf{R}_{m_k,o}}{\sum_{o' \in \mathcal{O}} \mathbf{R}_{m_k,o'} O_{o'}^{(g)}}.$$

m_k is the measurement corresponding to the k^{th} event of the group $N^{(g)}(o)$ is a normalization factor specific to the configuration of the g^{th} group taking into account the visibility of the o^{th} voxel. $\mathbf{R}_{m_k,o}$ is the probability to get a measurement in m_k, knowing an interaction in the object in the voxel o.

Because of the huge size of the matrix $\mathbf{R}$ representing the system model, its coefficients are computed on-the-fly instead of being stored. This computation is achieved by decomposing the model into three sub-models: the detector model, the collimator model, and the geometry model. More details on this reconstruction method are presented in [1].

III. Normalization

Normalization coefficients $N(o)$ correspond to the probability for a voxel to be detected by the system:

$$N(o) = \sum_m \mathbf{R}_{m,o}.$$

Its computation is more and more complex when increasing the number of possibilities of measurements m. Moreover, these normalization factors must be computed in real-time, before the reconstruction process.

To make this process fast enough, the model of the system is still considered as the succession of the detector model, the collimator model and the geometry model. Detector coefficients are obtained once for all the acquisitions. Non uniformity due to the detector is corrected before processing the measurements. Assuming that the variation of the sensitivity of the collimator evolves only with the distance from the source, the normalization of the collimation is solved using Monte Carlo sampling technique presented in [1]. Indeed, the retro-projection through the collimator is uniform with the depth. The non uniformity in depth is naturally corrected by picking retro-projected events uniformly among z axis.

Only the normalization factors relative to the geometry have to be computed after each re-configuration. Thus, the visibility of each voxel for the next configuration have to be calculated before the next reconstruction process begins. We refer to visibility as the amount of time spent on each head in such a position that the voxel is in the field of view:

$$N(o) = \sum_\alpha \sum_\beta t(\alpha,\beta) \times FOV_{\alpha,\beta}(o)$$

where $t(\alpha,\beta)$ is the time spent by α head in the β orientation, and $FOV_{\alpha,\beta}(o)$ is equal to 1 if the voxel o is in the field of view of the oriented head, 0 otherwise.

When the setup widely covers the imaged volume, this normalization map is quite uniform. But the normalization step becomes essential when the configuration is focused on a precise region of the volume.

The complexity of process can be represented by the number of calculation loops in the algorithm. Order of magnitude of complexities of real-time processes can not exceed those of the reconstruction process. The complexity of the reconstruction process c_{recons} depends on the number of event per group N_k, the number of voxels inside the volume of response $\mathcal{L}_m$ of a detection m, and slightly on the number of voxels representing the object ($\mathcal{O}$) in some special cases:

$$c_{recons} = N_k \times 2 \times card(\mathcal{L}_m)(+card(\mathcal{O})).$$

For the present configuration, its order of magnitude is 10^7.

Complexity of normalization c_{norm} process can be expressed as follows:

$$c_{norm} = N_\alpha \times N_t \times card(\mathcal{O}),$$

where N_α stands for the number of heads, and N_t is the number of time samples. Depending on the time sampling, the order of magnitude of this complexity is also 10^7. We thus consider that this process is calculable in real time.

IV. Configuring the Geometrical Parameters

As illustrated in Fig. 2, the adaptation process depends on a representative criteria of the information brought by each possible setup. This criteria must also be computed in real-time.

A. Fisher Information Matrix

The Fisher Information Matrix is often used to evaluate system designs [7]. It can be expressed as follow [8]:

$$F_{i,j} = \mathbf{E}\left[-\frac{\delta^2}{\delta O_i \delta O_j} \mathbf{ln} p(m|O)\right] = \sum_m \frac{\mathbf{R}_{m,i}\mathbf{R}_{m,j}}{\sum_b \mathbf{R}_{m,b} O_b},$$

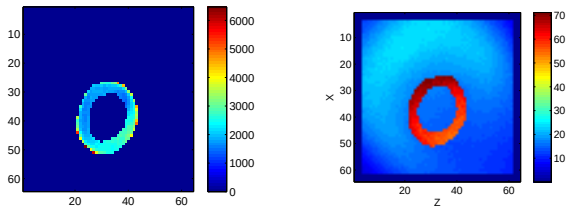

(a) (b)

Fig. 3. Fisher information on a myocard phantom with a cold background (a) and on a warm background (b)

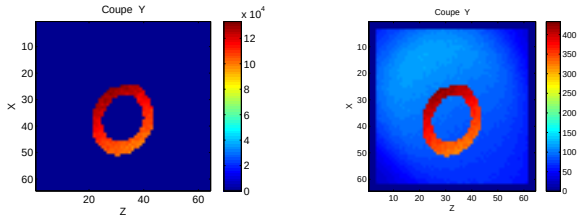

(a) (b)

Fig. 4. Information get from matrix DQE on a myocard phantom with a cold background (a) and on a warm background (b)

where i, j and b are voxels of the object, m is a measurement, and O is the supposed emitting object.

The computational load to get the Fisher Information Matrix is unmanageable in a context of 3D imaging. One commonly used method [9] consists in reducing the Fisher Information Matrix to its trace. Thus, covariance terms of a voxel with others are not calculated, and only its own variance is considered:

$$F_o = \sum_{m\in\mathcal{M}} \frac{\mathbf{R}_{m,o}^2}{\sum_{b\in\mathcal{O}} \mathbf{R}_{m,b} O_b}.$$

Finally, the information brought by one head α for a given orientation β about a specific object O correspond to the sum of products of information given by the setup on a voxel o by the activity O_o^2 of this voxel in the expected object:

$$i(\alpha,\beta) = \sum_{o\in\mathcal{O}} \sum_{m\in\mathcal{M}} \frac{\mathbf{R}_{m,o}^2}{\sum_{b\in\mathcal{O}} \mathbf{R}_{m,b} O_b} \times O_o^2.$$

$i(\alpha,\beta)$ is a precise criteria corresponding to the amount of information brought by the head α with β orientation about the expected object. Fig. 3 maps the distribution of the information on a myocard phantom, with a cold background and a warm background. It is thus possible to determine the most informative orientations for each head. The time spent on each orientation is adjusted depending on the score.

The complexity c_{Fisher} of the computation of Fisher information can be expressed as follows:

$$c_{Fisher} = N_\alpha \times N_\beta \times card(\mathcal{O}) \times 2 \times card(\mathcal{L}_m).$$

where N_β is the number of possible orientations for each head. In our context, the order of magnitude of this complexity is 2.10^{10}. Computed on the 8 cores of our i7-3770 CPU, it took 40 minutes.

It is thus necessary to use some approximations on this information in order to make the computation faster.

B. Detective Quantum Efficiency

One common approximation to evaluate the performance of a particular configuration of a gamma camera is the Detective Quantum Efficiency (DQE) [10]. It corresponds to the Fisher Information Matrix making the approximation that the source is uniform. Thus, the expression on this criteria is :

$$DQE_o = \sum_{m\in\mathcal{M}} \frac{\mathbf{R}_{m,o}^2}{\epsilon_m}.$$

where ϵ_m isthe sensitivity of the m^{th} measurement.

The information applied on a particular object is thus

$$i(\alpha,\beta) = \sum_{o\in\mathcal{O}} \sum_{m\in\mathcal{M}} \frac{\mathbf{R}_{m,o}^2}{\epsilon_m} \times O_o^2.$$

As it is noticeable on Fig. 4, this approximation is quite wrong when the background is cold, because the source is not uniform at all. But when the object is placed on a warm background, the distribution of information obtained with the DQE criteria is close from the one we get with the Fisher information. The approximation of the uniformity of the source is indeed less wrong. Moreover, the case of an object to detect on a warm background is more realist than an hot object on a cold background.

The computation of this criteria is twice faster than the criteria from Fisher Information :

$$c_{DQE} = N_\alpha \times N_\beta \times card(\mathcal{O}) \times card(\mathcal{L}_m).$$

Computed on 8 cores, it still takes about 20 minutes, that is still too long for our concern.

C. Analytic DQE

In order to make the criteria computation feasible online, matrix representation of the model is discarded. An analytic method to compute the DQE is proposed. Originally, the DQE is defined as the ratio between the output SNR on the input SNR. This can be rewrite in the following form [11] :

$$DQE_{\alpha,\beta} = \sum_a \epsilon_{\alpha,\beta} \times \sum_{n\in\mathcal{N}_a} PSF_{a,\alpha,\beta}^2(v),$$

where $\mathcal{N}_a$ is the neighbourhood of the voxel a. This neighboorhood is given by the spatial resolution of the head (α,β) for voxel a.

As illustrated in Fig. 5 , when considering the tangential variations of spatial resolution as negligible, spatial resolution Rs depends on the distance d between a voxel and the collimator:

$$Rs = t \times \frac{f+h+d}{f+h},$$

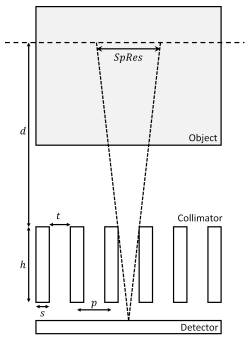

Fig. 5. Determination of the spatial resolution.

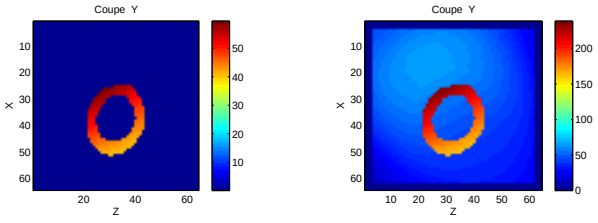

(a) (b)

Fig. 6. Information get from analytic DQE on a myocard phantom with a cold background (a) and on a warm background (b)

where t is the width of a hole, h is the collimator height, and f is the distance between the collimator and the detector.

Results obtained with this method are very close from those get with the matrix DQE, as illustrated on Fig. 6, but the computing is much faster.

The complexity c_{FoM} of the computing of this criteria is more advantageous than Fisher information:

$$c_{FoM} = card(\mathcal{O}) \times N_\alpha \times N_\beta \times card(\mathcal{N}),$$

as $card(\mathcal{N})$ is far smaller than $card(\mathcal{L}_m)$, the complexity deceases to 10^8. Its computation took only 20 seconds without parallelization.

V. Conclusion: benefits from adaptation on image quality

To conclude about the impact of the adaptation of the system on the result quality, we simulate nine points on a diagonal in the cubic object, quite close from each others (15 mm) in such a way that their distinction is at the limit of the performances of the chosen collimator. Two acquisitions was simulated. The first one was done with a classic configuration without any adaptation. The second one was adapted at the half of the acquiring time using the analytic DQE on the intermediate reconstruction. Estimations obtained are depicted on Fig. 7.

Points close from the camera (at the left on Fig. 7) are well distinguished for both acquisitions. There is a difference for points more distant from detectors. The initial acquisition fails in making the difference between two of them, whereas the acquisition with an adaptation does it well. Moreover,

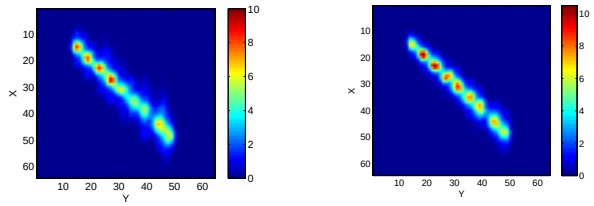

(a) (b)

Fig. 7. Estimations obtained with the basic configuration (a) an the adapted one (b).

the sensitivity of the adapted configuration is improved : for example in this case, we get 1.6 times more photons with the adapted configuration than with the other one.

Adapting the field-of-view during the examination is a way to enhances the trade-off between sensitivity and resolution, even through it implies real-time processing of both reconstruction and re-configuration. The configuration is adapted depending on the amount of information brought by each head and each orientation, in order to spend more time on the most relevant angles of each heads. The criteria used to determine an adapted configuration must be fast to compute. We proposed a criteria based on DQE feasible online. Finally, this work proved that this adaptation of the system could bring some enhancements on the image quality.

References

[1] M. Bernard, G. Montémont, S. Stanchina, L. Verger and S. Mancini, 20th Real Time Conference, IEEE TRPMS, to be published.

[2] G. Montémont, S. Lux, O. Monnet, S. Stanchina, and L. Verger, "Evaluation of a CZT gamma-ray detection module concept for SPECT," presented at the IEEE Nuclear Science Symposium Conference Record, 2012, pp. 4091–4097.

[3] G. Montemont, S. Lux, O. Monnet, S. Stanchina, and L. Verger, "Studying Spatial Resolution of CZT Detectors Using Sub-Pixel Positioning for SPECT," IEEE Transactions on Nuclear Science, vol. 61, no. 5, pp. 2559–2566, Oct. 2014.

[4] C. Robert, G. Montémont, V. Rebuffel, I. Buvat, L. Guérin, and L. Verger, "Simulation-based evaluation and optimization of a new CZT gamma-camera architecture," Phys. Med. Biol., vol. 55, no. 9, p. 2709, 2010.

[5] H. M. Hudson and R. S. Larkin, "Accelerated image reconstruction using ordered subsets of projection data," IEEE Trans Med Imaging, vol. 13, no. 4, pp. 601–609, 1994.

[6] H. H. Barrett, T. White, and L. C. Parra, "List-mode likelihood," J Opt Soc Am A Opt Image Sci Vis, vol. 14, no. 11, pp. 2914–2923, Nov. 1997.

[7] K. Vunckx, L. Zhou, S. Matej, M. Defrise, and J. Nuyts, "Fisher information-based evaluation of image quality for time-of-flight PET," IEEE Transactions on Medical Imaging, vol. 29, no. 2, pp. 311–321, 2010.

[8] H. H. Barrett, J. L. Denny, R. F. Wagner, and K. J. Myers, "Objective assessment of image quality. Ii. fisher information, fourier crosstalk, and figures of merit for task performance," Journal of the Optical Society of America, vol. 12, no. 5, pp. 834–852, 1995.

[9] J. Qi and R. M. Leahy, "Resolution and noise properties of MAP reconstruction for fully 3-D PET," IEEE Transactions on Medical Imaging, vol. 19, no. 5, pp. 493–506, 2000.

[10] S.-Å. Starck, M. Båth, and S. Carlsson, "The use of detective quantum efficiency (DQE) in evaluating the performance of gamma camera systems," Physics in Medicine and Biology, vol. 50, no. 7, pp. 1601–1609, 2005.

[11] G. Montemont, T. Bordy, V. Rebuffel, C. Robert, and L. Verger, "CZT pixel detectors for improved SPECT imaging," in 2008 IEEE Nuclear Science Symposium Conference Record, 2008, pp. 84–89.